Erratum: Quantum theory of light interaction with a Lorenz-Mie particle: Optical detection and three-dimensional ground-state cooling [Phys. Rev. A 108, 033714 (2023)]

Patrick Maurer, Carlos Gonzalez-Ballestero, and Oriol Romero-Isart

The phase factor $\exp(-2i\varphi_l^p)$ is missing in the expression for the information radiation pattern (IRP) in Eq. (A46), as the correct expression reads

$$\mathcal{I}_\mu(\theta_k, \phi_k) = \frac{\sum_g \left| \sum_{lmp} \bar{c}_{lmg}^{p*}(\theta_k, \phi_k) A_{lm}^{\mu p} \exp\left(-2i\varphi_l^p\right) \right|^2}{\sum_{lmp} \Theta(l - |m|) \left| A_{lm}^{\mu p} \right|^2}. \tag{1}$$

The expression for the recoil localization parameter Λ_μ is unaffected by this mistake. The phase is missing because we had derived the IRP for a photon that is inelastically scattered into a scattering eigenmode instead of a plane-wave mode, which is the relevant mode for optical detection along a given direction (θ_k, ϕ_k). As an additional justification for Eq. (1) one can show that the IRP corresponds to the normalized angular distribution of the rate of Fisher information $\mathcal{J}(r_\mu)$ delivered to the far field [1], that is,

$$\mathcal{I}_\mu(\theta_k, \phi_k) = \frac{1}{\int d\mathcal{J}(r_\mu)} \frac{d\mathcal{J}(r_\mu)}{d\Omega_k}. \tag{2}$$

The correct IRP differs from the original IRP mainly along $\mu = z$ and for sufficiently large particles but all main conclusions remain unaffected by this correction.

List of changes

To be consistent with the above correction, the original paper must be updated according to the following list of changes.

(i) Replace $A_{lm}^{\mu p} \to A_{lm}^{\mu p} \exp(-2i\varphi_l^p)$ in Eq. (A39) and Eq. (A46).

(ii) Replace $\hat{a}_\kappa^\dagger \to \hat{b}_\kappa^\dagger$ in the definition of the output states $|\Psi_{\text{out}}^p\rangle$ throughout the text, where $\hat{b}_\kappa^\dagger$ is the creation operator of a normalized plane-wave mode with mode multi-index κ. The correct IRP in Eq. (1) can then be derived following the steps of the original paper and using $\lim_{T \to \infty}[\hat{b}_\kappa(T) \exp(i\omega_\kappa T)] = \sum_{\kappa'} S_{\kappa\kappa'} \hat{a}_{\kappa'}$, where $\hat{b}_\kappa(t)$ denotes the plane-wave annihilation operator in the interaction picture and $S_{\kappa\kappa'}$ denotes the single-photon scattering matrix [2].

(iii) Replace $G_{\kappa\mu} \to \sum_{\kappa'} S_{\kappa\kappa'} G_{\kappa'\mu}$ in Eq. (22), Eqs. (A34) and (A35), the text between Eq. (A37) and Eq. (A38), Eq. (A38) itself, and in the numerator of Eq. (A46).

(iv) Replace Figs. 4 and 5, Figs. 7 and 8, and Figs. 10 and 11 with the following updated figures and make minor changes to the text to reflect the results in the updated figures.
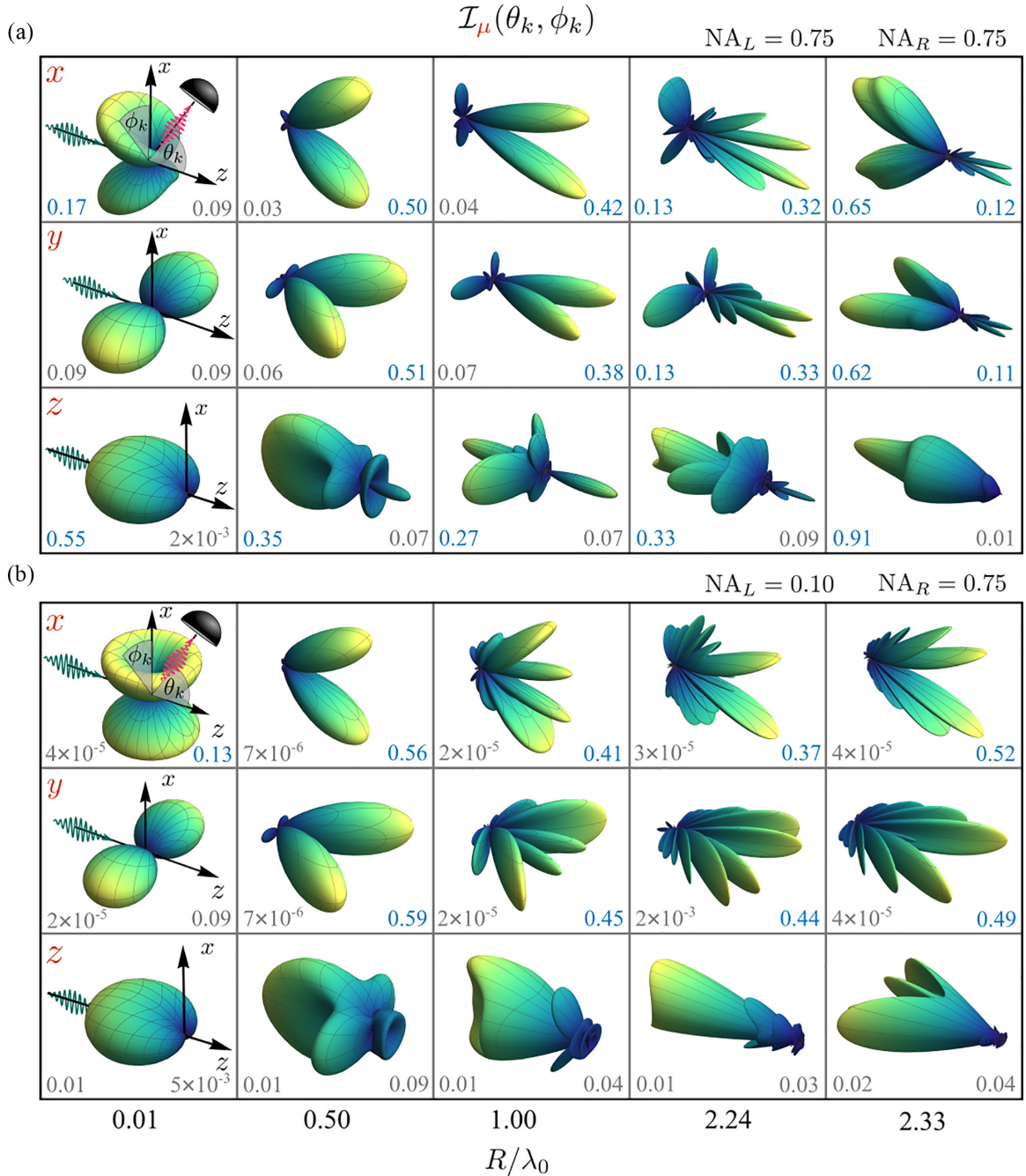
FIG. 4. Updated Fig. 4 of the original paper. Information radiation patterns $\mathcal{I}_\mu(\theta_k, \phi_k)$ of a silica sphere and a single focused x-polarized Gaussian beam propagating along the positive z axis (reference frame in first row). The value of the IRP is encoded both in the radial distance from the center and the color scale. The focusing lens has a numerical aperture $NA_L = 0.75$ in panel (a) and $NA_L = 0.10$ in panel (b), while the collection lens has a numerical aperture $NA_R = 0.75$ in both panels. The detection efficiency for the focusing lens and collection lens is shown in each subpanel (highlighted in blue for $\eta_\mu^d > 1/9$). Across panels the value of R/λ_0 is, for each column, constant and indicated below the last row.
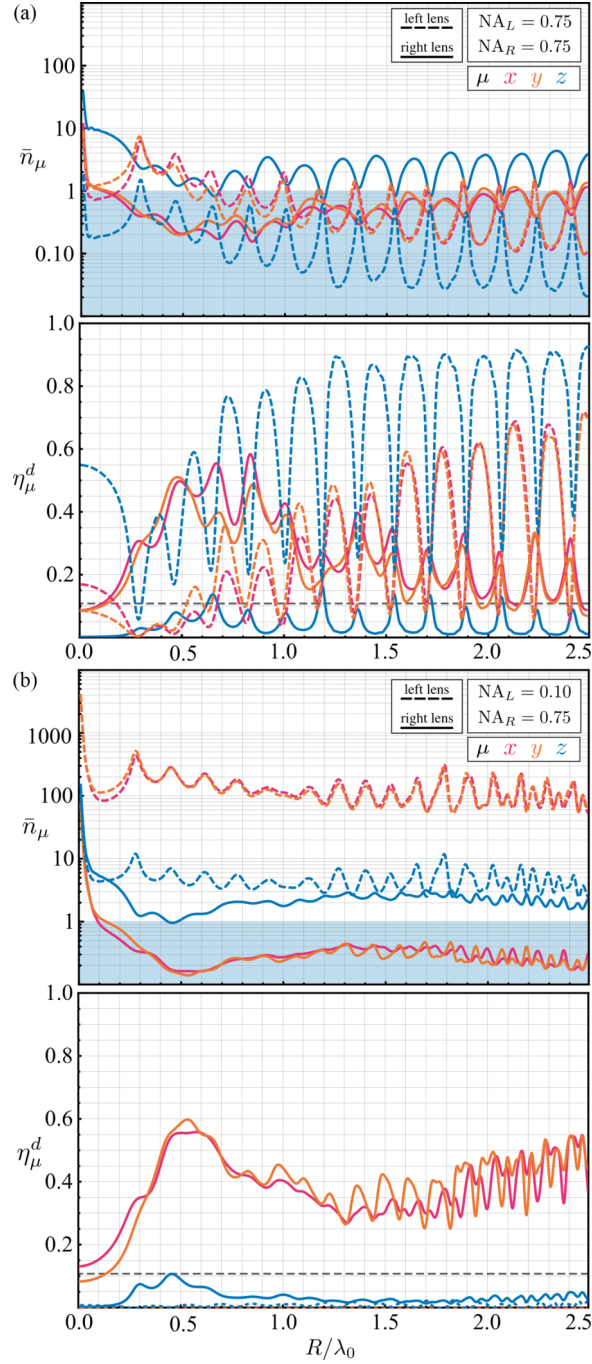
FIG. 5. Updated Fig. 5 of the original paper. Detection efficiencies η_μ^d and minimum achievable mean phonon occupation number $\bar{n}_\mu$ along x, y, and z for ideal feedback as a function of R/λ_0 and $p = 10^{-9}$ mbar, $T = 300$ K, at the same optical configuration as in Fig. 3 in the original paper. The dashed (solid) lines correspond to the values at the left (right) lens. The blue shaded area highlights the region where $\bar{n}_\mu < 1$ and the gray dashed line shows $\eta_\mu^d = 1/9$, respectively.
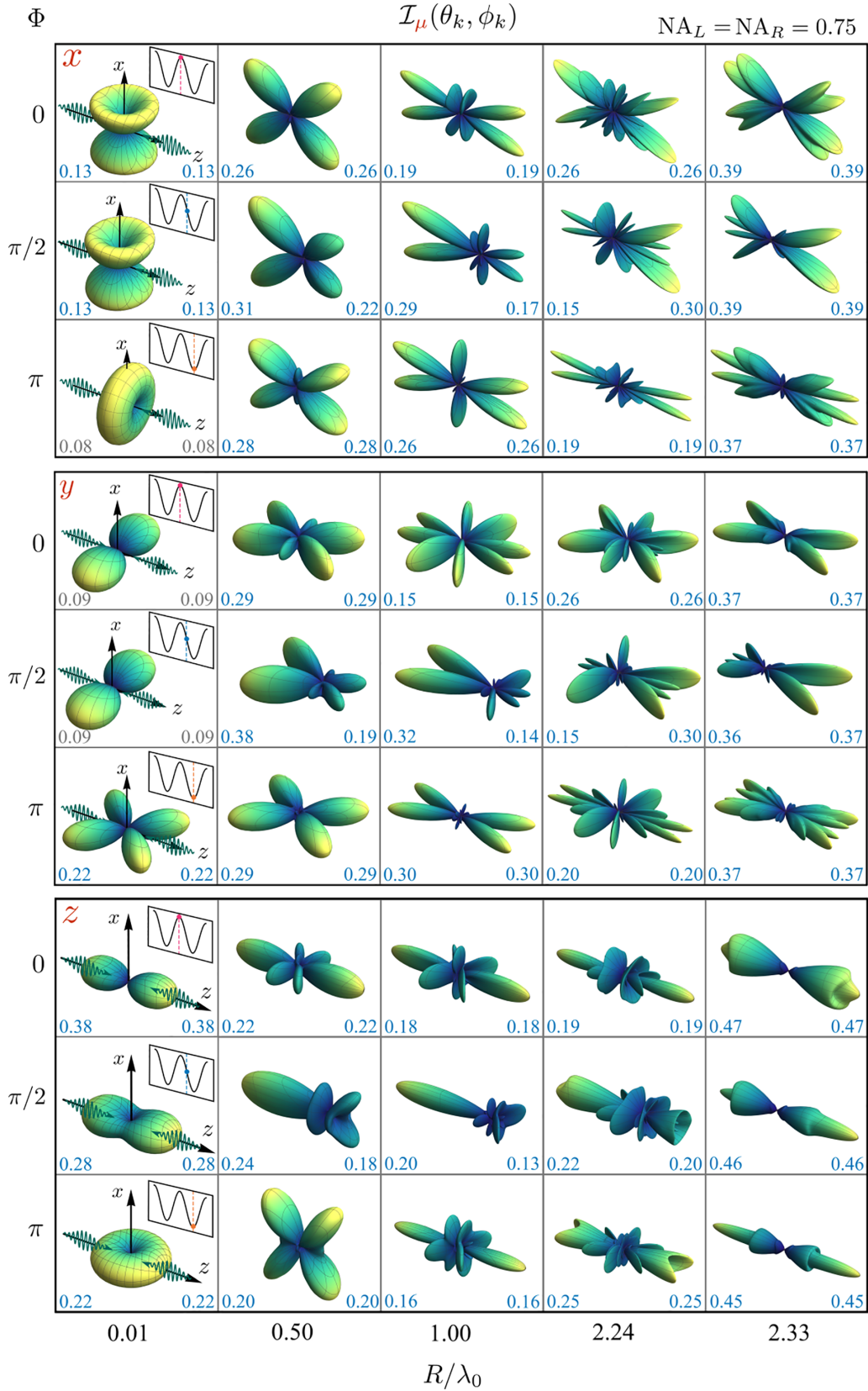
FIG. 7. Updated Fig. 7 of the original paper. Information radiation patterns $\mathcal{I}_\mu(\theta_k, \phi_k)$ of a silica sphere, two focused x-polarized Gaussian beams counterpropagating parallel to the z axis (reference frame in first row), and relative phases $\Phi = 0, \pi/2, \pi$ (corresponding intensity at origin shown as inset in first column). The value of the IRP is encoded both in the radial distance from the center and the color scale. The two focusing lenses have a numerical aperture $\mathrm{NA}_L = \mathrm{NA}_R = 0.75$. The detection efficiency for the left and right lens shown in each subpanel (highlighted in blue for $\eta_\mu^d > 1/9$). Across panels the value of R/λ_0 is, for each column, constant and indicated below the last row.
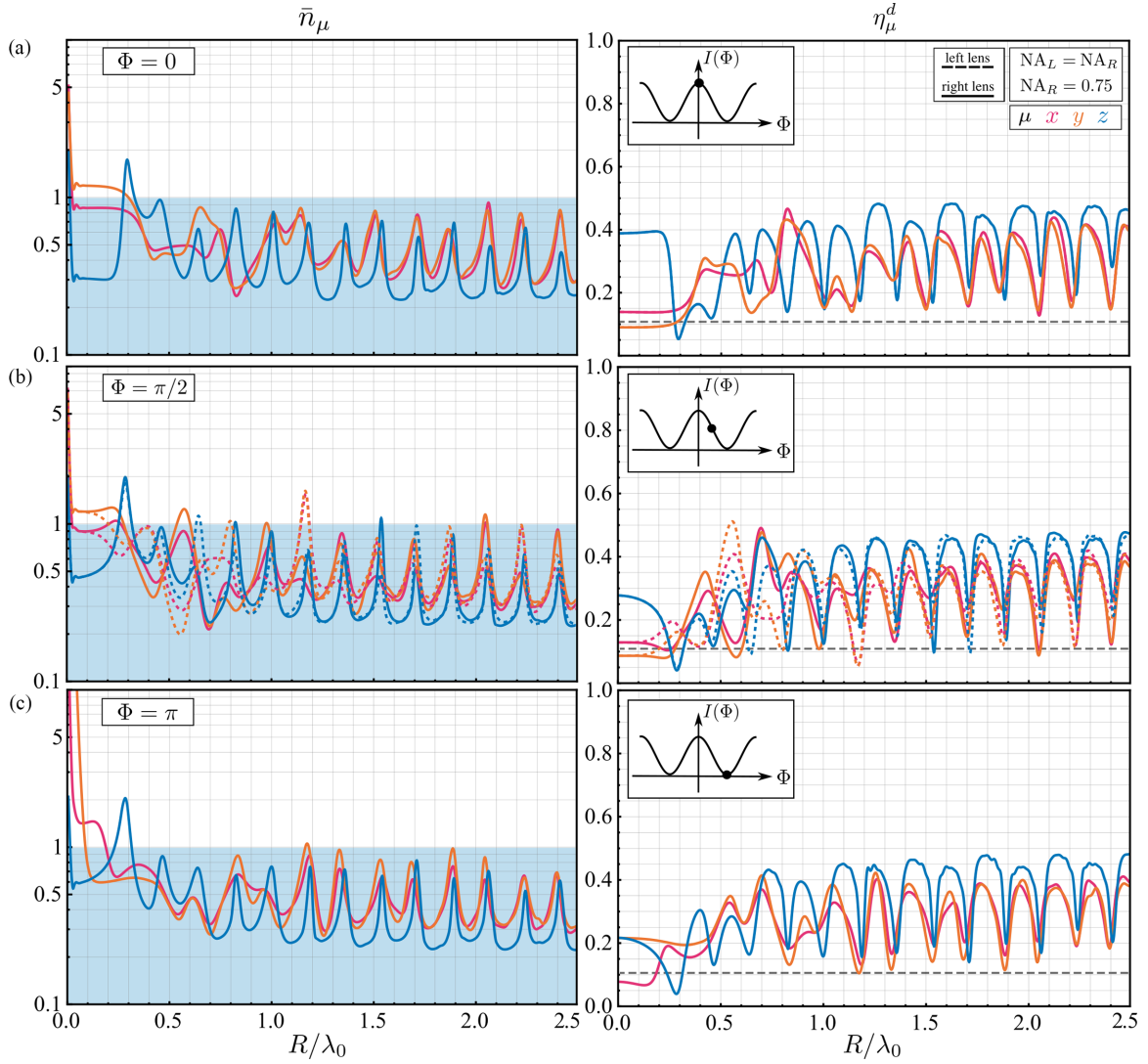
FIG. 8. Updated Fig. 8 of the original paper. Detection efficiencies η_μ^d and minimum achievable mean phonon occupation number $\bar{n}_\mu$ along x, y, z for ideal feedback as a function of R/λ_0 and $p = 10^{-9}$ mbar, $T = 300$ K, at the same optical configuration as in Fig. 7, where panels (a)–(c) correspond to $\Phi = 0, \pi/2, \pi$ with an inset that maps the relative phase Φ to the corresponding intensity at the origin. The dashed (solid) lines correspond to the values at the left (right) lens. The blue shaded area highlights the region where $\bar{n}_\mu < 1$ and the gray dashed line shows $\eta_\mu^d = 1/9$, respectively.
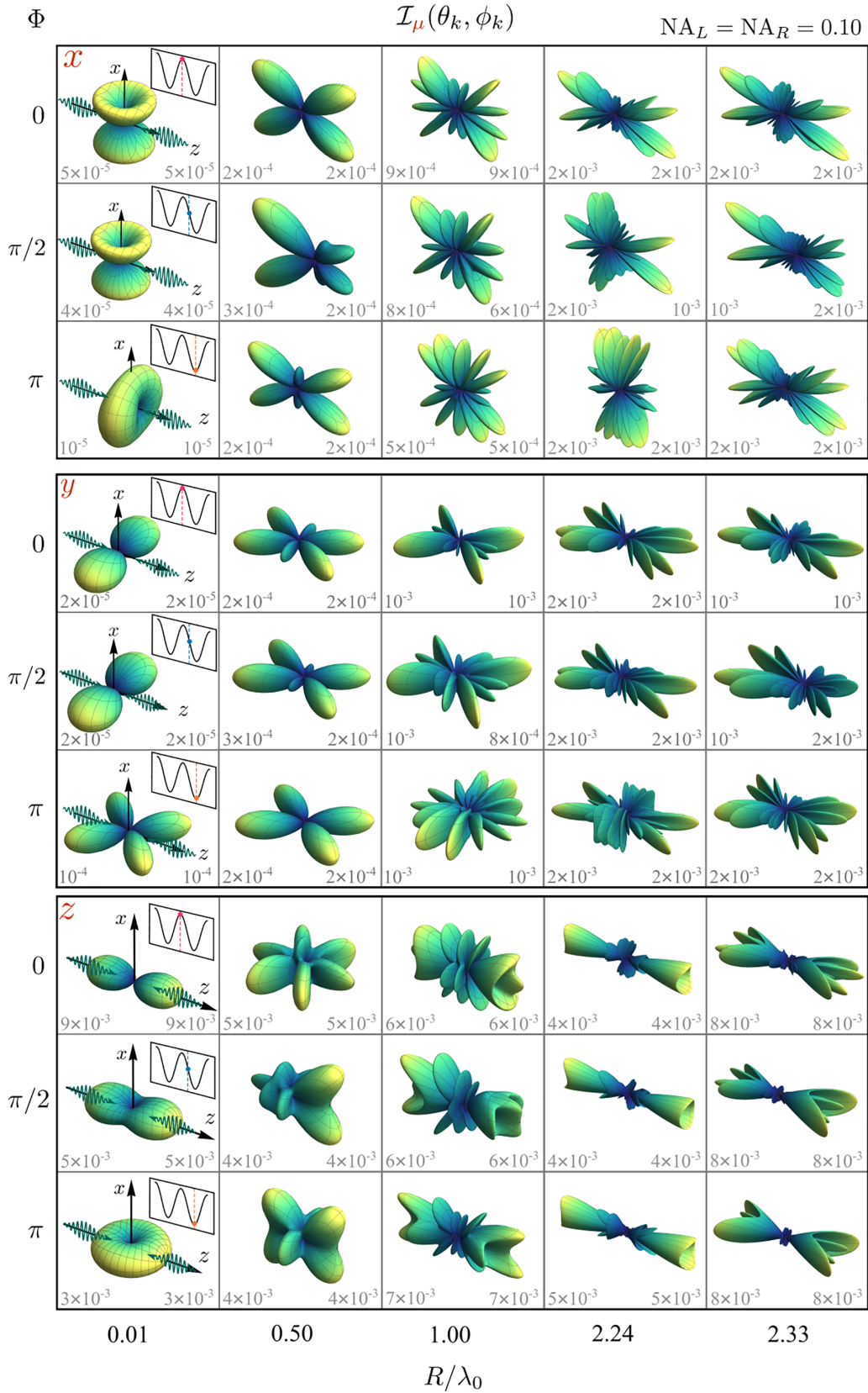
FIG. 10. Updated Fig. 10 of the original paper. Information radiation patterns $\mathcal{I}_\mu(\theta_k, \phi_k)$ of a silica sphere, two focused x-polarized Gaussian beams counterpropagating parallel to the z axis (reference frame in first row), and relative phases $\Phi = 0, \pi/2, \pi$. The value of the IRP is encoded both in the radial distance from the center and the color scale. The two focusing lenses have a numerical aperture $\mathrm{NA}_L = \mathrm{NA}_R = 0.10$. The detection efficiency for the left and right lens is shown in each subpanel (highlighted in blue for $\eta_\mu^d > 1/9$). Across panels the value of R/λ_0 is, for each column, constant and indicated below the last row.
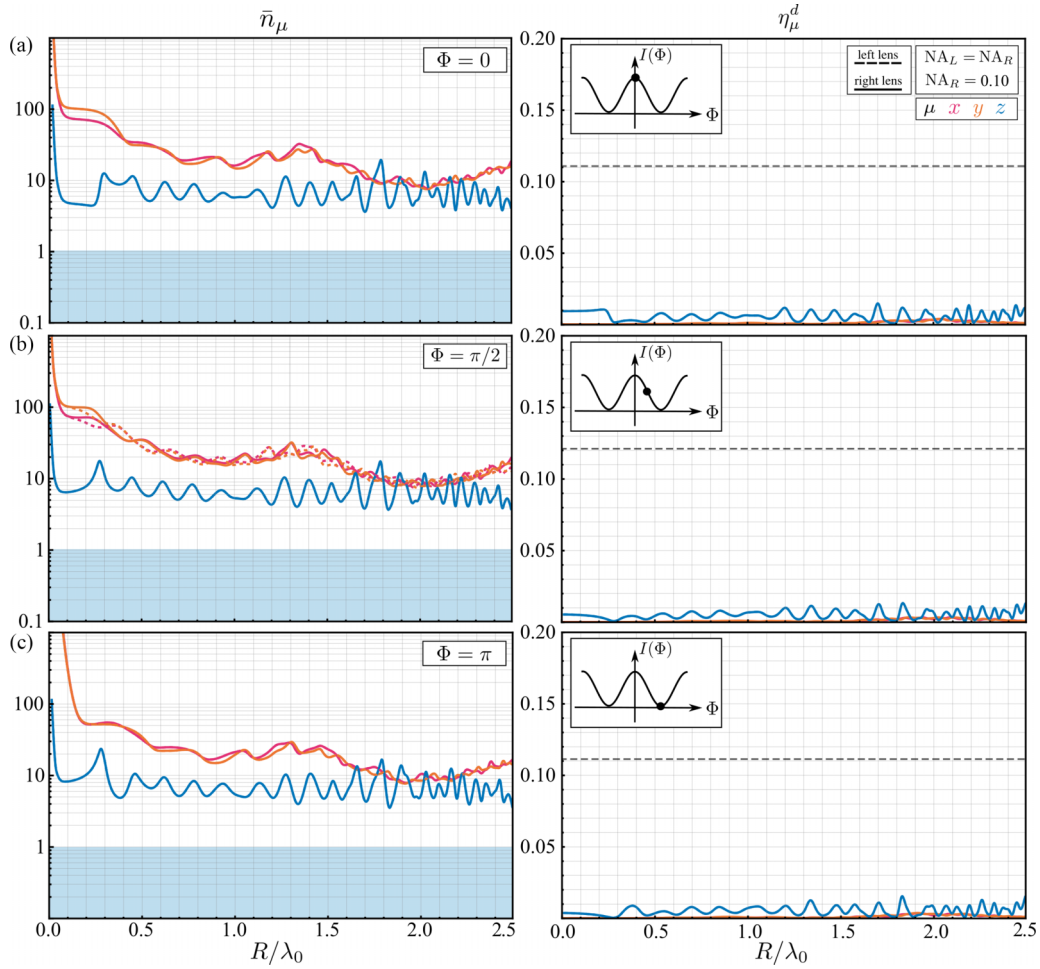
FIG. 11. Updated Fig. 11 of the original paper. Detection efficiencies η_μ^d and minimum achievable mean phonon occupation number $\bar{n}_\mu$ along x, y, z for ideal feedback as a function of R/λ_0 and $p = 10^{-9}$ mbar, $T = 300$ K, at the same optical configuration as in Fig. 9 in the original paper, where panels (a)–(c) correspond to $\Phi = 0, \pi/2, \pi$ with an inset that maps the relative phase Φ to the corresponding intensity at the origin. The dashed (solid) lines correspond to the values at the left (right) lens. The blue shaded area highlights the region where $\bar{n}_\mu < 1$ and the gray dashed line shows $\eta_\mu^d = 1/9$, respectively.

[1] J. Hüpfl, F. Russo, L. M. Rachbauer, D. Bouchet, J. Lu, U. Kuhl, and S. Rotter, Continuity equation for the flow of Fisher information in wave scattering, arXiv:2309.00010.

[2] P. Maurer, C. Gonzalez-Ballestero, and O. Romero-Isart, Quantum electrodynamics with a nonmoving dielectric sphere: Quantizing Lorenz–Mie scattering, J. Opt. Soc. Am. B **40**, 3137 (2023).